Journal of Alloys and Compounds, 189 (1992) 175–186
JALCOM 354

Investigation of thermodynamic properties of the Ti–H system using molten salt electrolytes containing hydride ions

Bor Yann Liaw*, Gerhard Deublein and Robert A. Huggins
Department of Materials Science and Engineering, Stanford University, Stanford, CA 94305 (USA)

(Received August 27, 1991; in final form April 28, 1992)

Abstract

A novel molten salt technique using alkali halide electrolytes, which contain hydride ions, was used to study thermodynamic properties of the Ti–H system at intermediate temperatures (300–415 °C). This electrochemical technique offers a simple, fast, precise and sensitive method for investigation of metal–hydrogen interactions with minimal surface interference at temperatures where no suitable electrolyte was available previously. We report results that extend to a lower hydrogen activity range than any previous studies. The results agree with those measured by others using conventional gas-volumetric or calorimetric techniques.

1. Introduction

A novel molten salt technique is described here to illustrate its applicability to the investigation of metal–hydrogen interactions. Many metal–hydrogen systems exhibit great potential for future hydrogen-based energy-related applications. These systems can be used as hydrogen storage media [1–4]; as electrode materials in chemical sensors [5], batteries and fuel cells; as filters in hydrogen purification; and as catalysts for hydrogenation or dehydrogenation.

The Ti–H system has long been considered a useful hydrogen storage medium [2, 6, 7]. Many researchers have studied this system using the gas-volumetric absorption method. Earlier work by Kirschfeld and Sieverts [8] determined some aspects of the pressure–composition–temperature (p–c–T) relationships. McQuillan [9] reported an established binary phase diagram in the early 1950s with more detailed p–c–T and other thermodynamic information. Gibb and coworkers [10, 11] conducted equilibrium hydrogen partial pressure measurements that extended to both low and high pressure ranges. They reported a marked difference in their measurements due to the effect of impurities. Haag and Shipko [12] further studied the p–c–T behaviors in low pressure and temperature regions. Mueller *et al.* [7] reviewed the binary Ti–H system up to 1968. Nagasaka and Yamashina [13] subsequently studied hydrogen solubility under ultrahigh vacuum conditions. Arita *et al.* [14] and, later, Dantzer [15] investigated the thermodynamic properties of the Ti–H system, including information on equilibrium hydrogen partial pressure, standard free energy of formation of binary phases, enthalpy and entropy change of hydride formation [14] and partial molar enthalpy and entropy of mixing [15]. Veleckis and Rogers [16] measured the p–c–T relationships in the α and $\alpha+\beta$ phase regions between 370 and 860 °C. Most recently, San-Martin and Manchester [17] presented a modified phase diagram (Fig. 1) with detailed crystal structure and ther-

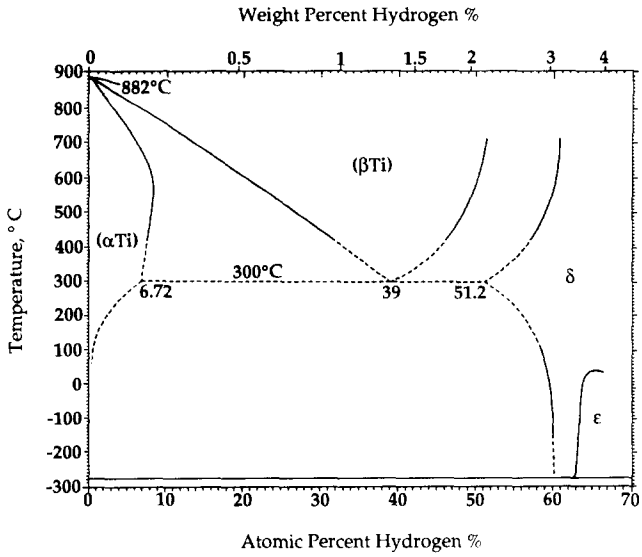

Fig. 1. Binary Ti–H phase diagram (after ref. 17).

*Author to whom correspondence should be addressed. Present address: Hawaii Natural Energy Institute, School of Ocean and Earth Science and Technology, University of Hawaii, 2540 Dole St., Holmes Hall 246, Honolulu, HI 96822, USA.

0925-8388/92/$5.00

modynamic information collected from an extensive literature survey.

The conventional gas-volumetric absorption technique is quite limited in both high and low pressure regimes because of experimental complexity and difficulty in experimental control. We can overcome this shortcoming by both employing a molten salt electrolyte containing alkali hydride in an electrochemical cell and using electrochemical techniques to study the metal–hydrogen systems. An example is the use of organometallic molten salts, $NaAl(C_2H_5)_4$, containing NaH in the study of ternary Mg–(Ni,Cu)–H systems, as reported by Lüdecke *et al.* [18–20].

A new approach using eutectic LiCl–KCl or LiI–KI molten salts containing LiH to investigate the thermodynamic properties of the Ti–H system is presented here. Deublein and Huggins [21] have shown that excess LiH dissolved in the alkali halide melt creates an environment of extremely low water and oxygen activity, with which surface metal oxides are no longer stable. The metal oxides react with excess LiH to form soluble lithium oxide and hydrogen gas, producing a "hydrogen-transparent", clean metal surface *in situ*. The dissolved LiH also provides Li^+ and H^- as the conducting species, and the latter is different from more commonly used proton (H^+) conductors.

This unique H^--conducting electrolyte system can be readily employed with precise and sensitive electrochemical techniques to investigate the metal–hydrogen interactions without the influence of impeding surface oxide layers. We have obtained quantitative results using equilibrium coulometric titration techniques [22] and determined compositional thermodynamic properties of the Ti–H system using simple electrochemical cells at 300, 355 and 415 °C.

2. Experimental details

2.1. Experimental set-up and coulometric titration techniques

A typical electrochemical cell is illustrated in Fig. 2. A titanium plate attached to a molybdenum current collector was used as the positive electrode (anode). An aluminum rod was used as the negative electrode (cathode). The Li^+ ions in the melt reacted easily with the aluminum to form nominal Li–Al alloys, while the H^- reacted with the titanium to form hydride phases. Two types of reference electrodes were used. One was a two-phase α-Al/β-"LiAl" alloy, which, with the LiH dissolved in the melt, constituted a secondary hydrogen electrode. The other was a two-phase α-Ti/β-"TiH_x" alloy (or an α-Ti/δ-"TiH_x" mixture if below the eutectoid temperature), which served as a primary hydrogen reference electrode [5]. Both reference electrodes were

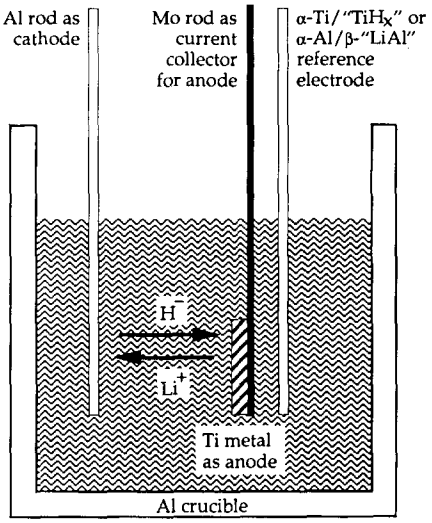

Fig. 2. Experimental set-up of the electrochemical cell. A eutectic LiI–KI melt containing LiH was used as the electrolyte at 300 and 355 °C and a eutectic LiCl–KCl melt containing LiH was used at 415 °C. The "TiH_x" phase in the reference electrode denotes the nominal δ phase below the eutectoid temperature in the Ti–H system and the β phase above such a temperature.

made by electrochemically decomposing LiH in the melt and subsequently allowing the following two reactions to occur simultaneously: lithium reacted with the aluminum rod to form an α-Al/β-"LiAl" two-phase mixture and hydrogen reacted with the titanium rod to produce an α-Ti/β-"TiH_x" (or α-Ti/δ-"TiH_x" if below the eutectoid temperature) two-phase mixture—which were the same as the half-cell reactions of interest.

The coulometric titration curves were obtained by galvanostatically adding known amounts of charge into the titanium metal intermittently. The accumulated charge was equated to the amount of hydrogen in the titanium by

$$xH^- + Ti = TiH_x + xe^- \quad (1)$$

if hydrogen evolution was carefully avoided. The equilibrium open-circuit voltage (OCV) *vs.* 1 atm hydrogen was then measured as a function of composition (in terms of the H:Ti ratio x). The relationship of OCV and hydrogen activity (a_H) in the sample was given by the Nernst equation

$$OCV = \mathscr{E}^\circ = -\frac{RT}{zF} \ln a_H \quad (2)$$

where R, T, z and F have their usual meanings and $\mathscr{E}^\circ$ is the electrochemical potential *vs.* a standard hydrogen electrode to be described in Section 2.2.

In a binary system the Gibbs phase rule constrains the component (*i.e.* titanium and hydrogen) activities to be constant if two phases are in equilibrium under constant temperature and pressure. A constant plateau potential will thus appear in the two-phase region on the titration curve. Otherwise, the respective component

activity, and thus its corresponding electrochemical potential, will vary with composition. This rule can be used to determine the phase boundaries in a binary system.

The coulometric titration results provide the basis for further calculation of the thermodynamic properties of the metal–hydrogen system. We will discuss the relationship between the coulometric titration results and the thermodynamic properties in Section 2.3.

2.2. Measuring temperature-dependent plateau potential

A series of experiments were designed to obtain the plateau potential as a function of temperature. The experiments measured the α-Ti/β-"TiH_x" plateau potential against a Pd/H_2(g) (at 1 atm) reference electrode in the temperature range 350–400 °C. The Pd/H_2 electrode was in contact with pure hydrogen at 1 atm and therefore was considered as a standard hydrogen electrode, SHE*, which corresponded to the reversible reaction

$$H^- = \tfrac{1}{2}H_2 + e^- \tag{3}$$

The measured temperature variation of the plateau potential correlated the coulometric titration results to the standard state and was used to calculate the reaction entropy change of the α-to-β-hydride phase transformation as discussed in Section 2.3.5.

2.3. Thermodynamic quantities

The results from these electrochemical measurements were used to determine thermodynamic properties of the Ti–H system. The following section explains the relationship between the electrochemical quantities and the thermodynamic properties.

2.3.1. Free energies

The Gibbs free energy of formation for TiH_x in the system was obtained by integrating the area above the coulometric titration curve, in which the potential $\mathscr{E}^\circ$ was measured *vs.* a standard hydrogen electrode, SHE*, to the desired composition x in reaction (1):

$$\Delta G_f^\circ(TiH_x) = -zF\int_0^x \mathscr{E}^\circ \, dx \tag{4}$$

This quantity is based on per mole of TiH_x produced. The integral molar free energy of mixing per mole of titanium was then

$$\Delta G_m = \frac{\Delta G_f^\circ(TiH_x)}{1+x} \tag{5}$$

The partial molar free energy of mixing per mole of hydrogen in TiH_x was depicted by the Nernst equation as

$$\Delta G_H = RT \ln a_H = -zF\mathscr{E}^\circ \tag{6}$$

The partial molar free energy of mixing per mole of titanium in TiH_x was thus

$$\Delta G_{Ti} = -zF\left(\int_0^x \mathscr{E}^\circ \, dx - \mathscr{E}^\circ x\right) \tag{7}$$

When hydrogen solution in the single-phase region was considered, the free energy of mixing had the same meaning as the free energy of solution or dissolution.

The integration of the area above a two-phase plateau, which exemplifies a hydride (such as α-to-β) transformation,

$$\text{"}TiH_x\text{"} + \frac{y}{2}H_2 = \text{"}TiH_{x+y}\text{"} \tag{8}$$

gave the free energy of reaction (*i.e.* α-to-β transformation)

$$\Delta G_r^\circ = -zF\int_x^{x+y} \mathscr{E}^\circ \, dx \tag{9}$$

on the basis of one mole of "TiH_x" (*i.e.* α phase) or $y/2$ moles of H_2 (or y moles of H). "TiH_x" (*i.e.* α phase) and "TiH_{x+y}" (i.e. β phase) represent the upper limit of composition in the low hydrogen content (α) phase and the lower limit of composition in the high hydrogen content (β) phase respectively.

2.3.2. Activities

The hydrogen activity in metals or hydrides was calculated from the measured electrochemical potential $\mathscr{E}^\circ$ using the Nernst equation expressed in (2) or (6). The corresponding titanium activity in TiH_x can be calculated by

$$a_{Ti} = \exp\left(-\frac{zF\left(\int_0^x \mathscr{E}^\circ \, dx - \mathscr{E}^\circ x\right)}{RT}\right) \tag{10}$$

The activity varies with the composition parameter x (the H:Ti ratio) in the single-phase region as depicted by the Gibbs phase rule for constant temperature and pressure.

2.3.3. Sieverts' constant

Sieverts' law expresses the linear relationship between the hydrogen activity and its concentration by Sieverts' constant K_s:

$$(P_{H_2})^{1/2} = a_H = K_s(H{:}Ti) = K_s x \tag{11}$$

This relationship is usually valid in the low hydrogen concentration region, similar to Henry's law that applies in solutions with dilute solute.

2.3.4. Enthalpies

The above Sieverts relationship can also be expressed by an exponential equation [13, 23]

$$a_H = k \exp\left(\frac{\Delta H_H}{RT}\right)(\text{H:Ti}) \tag{12}$$

$$K_s = k \exp\left(\frac{\Delta H_H}{RT}\right) \tag{13}$$

where k is a pre-exponential constant related to the entropy change and ΔH_H is the partial molar enthalpy of mixing for hydrogen solution. From (13) we can derive a relation between K_s and T in order to obtain ΔH_H:

$$\log K_s = \frac{\Delta H_H}{2.303RT} + \log k \tag{14}$$

If a curve of $\log K_s$ *vs.* $1/T$ is plotted, the slope of such a curve gives ΔH_H and the intercept determines k.

Equation (14) can also be derived from eqns. (6) and (11). Introducing (11) into (6), we may write

$$\Delta G_H = RT \ln a_H = RT \ln(K_s x) = RT \ln K_s + RT \ln x \tag{15}$$

while

$$\Delta H_H = \Delta G_H + T \Delta S_H \tag{16}$$

The partial molar entropy of mixing for hydrogen, ΔS_H, can be attributed to two parts: one is associated with the configurational entropy change, as depicted by $-R \ln[x/(1-x)]$, due to compositional variation, while the other relates to the interaction of hydrogen with the metal lattice during dissolution, $-R \ln(1-x) - R \ln k$, which includes the accompanied volume change, *i.e.*

$$\Delta S_H = -R \ln x - R \ln k \tag{17}$$

We therefore obtain a similar equation to (13):

$$\Delta H_H = RT \ln K_s - RT \ln k \tag{18}$$

$$K_s = k \exp\left(\frac{\Delta H_H}{RT}\right) \tag{19}$$

2.3.5. Entropies

The entropy change of reaction (8) can be obtained by the relationship

$$\Delta S_r^\circ = -\frac{\partial \Delta G_r^\circ}{\partial T} = zF \frac{\partial \mathscr{E}^\circ}{\partial T} \tag{20}$$

Thus, by measuring the temperature dependence of the reaction plateau potential and from the slope of such a plateau potential *vs.* temperature curve ($\partial \mathscr{E}^\circ / \partial T$), we can determine ΔS_r° through (20). The corresponding enthalpy change ΔH_r° can then be calculated using

$$\Delta H_r^\circ = \Delta G_r^\circ + T \Delta S_r^\circ \tag{21}$$

On the other hand, the partial molar entropy of mixing for hydrogen, ΔS_H, can be obtained from

$$\Delta S_H = \frac{\Delta H_H - \Delta G_H}{T} \tag{22}$$

where ΔG_H was determined in (6) and ΔH_H came from (14).

In the low hydrogen content solid solution region where Sieverts' law applies, we also measured the temperature dependence of the electrochemical potentials. This measurement provided the data for further interpolation of the free entropy change of formation (hydrogen solution) per mole of TiH_x, $\Delta S_f^\circ(TiH_x)$, and the integral molar entropy change of mixing per mole of titanium, ΔS_m, where

$$\Delta S_f^\circ(TiH_x) = zF \int_0^x \frac{\partial \mathscr{E}^\circ}{\partial T} \, dx \tag{23}$$

$$\Delta S_m = \frac{\Delta S_f^\circ(TiH_x)}{1+x} \tag{24}$$

Likewise, we can calculate the partial molar entropy of mixing for hydrogen solution in the single-phase region from

$$\Delta S_H = zF \frac{\partial \mathscr{E}^\circ}{\partial T} \tag{25}$$

and compare with those obtained from (22). In a similar vein we may use (22) and ΔS_H from (25) to calculate ΔH_H for further comparison with that determined from (14). Results obtained from these alternative calculations should be consistent with each other.

3. Results

3.1. Coulometric titration curves

Figure 3 shows the measured coulometric titration curves of the Ti–H system at 300, 355 and 415 °C in comparison with data extracted from the *p–c–T* curves reported in ref. 17 at 303, 404 and 427 °C. For the data measured at 300 °C the OCV changes from −458 to −362 mV in the α-Ti solid solution region, where the hydrogen content varies from H:Ti ≈ 0.006 to H:Ti ≈ 0.079. A two-phase $\alpha+\delta$ plateau occurs thereafter at −362 mV and the H:Ti ratio extends from 0.079 to less than 1.013, where small potential increments start to be noticed until H:Ti ≈ 1.5. After H:Ti = 1.5 a

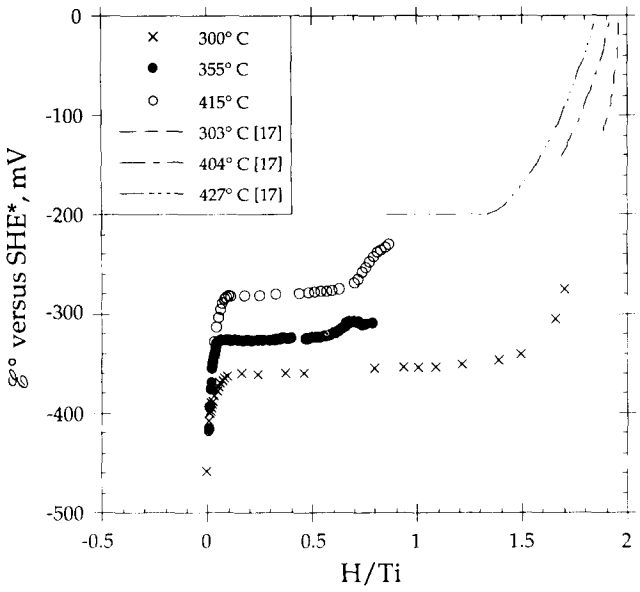

Fig. 3. Equilibrium coulometric titration curves of the Ti–H system at 300, 355 and 415 °C, which show a good correspondence with the existing phase diagram (Fig. 1). Dashed lines are interpolated from data extracted from the *p–c–T* curves reported by San-Martin and Manchester [17] at 303, 404 and 427 °C.

much larger compositional dependence of the potential was measured. Presumably the potential would have increased to what corresponds to 1 atm hydrogen if the experiments were conducted further.

The curves at 355 and 415 °C behave quite differently: the single $\alpha+\delta$ plateau has been replaced by two two-phase plateaux; a new β-hydride phase appears and the first and second plateaux are due to $\alpha+\beta$ and $\beta+\delta$ equilibria.

At 355 °C the equilibrium OCV varies from −416 to −327 mV in the α solid solution region. The corresponding composition change is from H:Ti ≈ 0.010 to H:Ti = 0.063. The first plateau of $\alpha+\beta$ appears at −327 mV, ranging from H:Ti = 0.063 to H:Ti = 0.53. In the composition range H:Ti = 0.53–0.74 the OCV increases from −327 to −310 mV with increasing hydrogen concentration. This is the β-hydride phase region. A second plateau of $\beta+\delta$ occurs at −310 mV.

The curve at 415 °C shows that the OCV in the α solid solution region changes from −418 to −280 mV for $0.009 \leqslant$ H:Ti < 0.085. The two-phase $\alpha+\beta$ region has a plateau potential of −280 mV in the range $0.085 <$ H:Ti $\leqslant 0.48$. In the region $0.485 <$ H:Ti < 0.63 the potential changes are small but noticeable. After H:Ti > 0.65 the potential in the β-hydride phase region starts to increase appreciably up to H:Ti ≈ 0.87, where the second plateau starts to appear at about −230 mV. Presumably this is the plateau potential of the two-phase $\beta+\delta$ region.

3.2. Phase boundaries

From the coulometric titration curves we can determine the phase boundaries for different phases in the system. These phase boundary limits are listed in Table 1 for comparison with values reported by others [9, 15, 17, 24–28].

3.3. Initial hydrogen concentration

Within the α phase solid solution region we are interested in studying the Sieverts' law relationship to determine values of Sieverts' constant. When the hydrogen activity determined from (6) was plotted against the amount of hydrogen electrochemically introduced into the sample, a linear relationship was obtained in the low concentration region, as expected from Sieverts' law. Figure 4 displays the curve for 415 °C as an example. This curve, however, did not pass through the origin as would be expected, but intercepted with the vertical axis at an activity $a_H{}^*$ for zero hydrogen content introduced. We assumed that this activity comes

TABLE 1. Phase boundaries of different phases in the Ti–H system

Phase boundary	Composition (H:Ti)	T (°C)	Reference(s)
$\alpha/(\alpha+\beta)$	0.086	441	[17, 24]
	0.077	404	[17, 25]
	0.071	337	[17, 25]
	0.084	415	[9]
	0.083	355	[9]
	0.0915	464–473	[15]
	0.063	355	This work
	0.085	415	
$(\alpha+\beta)/\beta$	0.442	441	[17, 24]
	0.486	415	[9]
	0.569	355	[9]
	0.51	473	[15]
	0.42	464	[15]
	0.53	355	This work
	0.48	415	
$\beta/(\beta+\delta)$	0.890	441	[17, 24]
	0.878	427	[17, 26]
	0.884	415	[9]
	0.915	464–473	[15]
	0.74	355	[17]
	0.74	355	This work
	0.87	415	
$\alpha/(\alpha+\delta)$	0.076	319	[17, 27]
	0.062	300	[17, 27]
	0.051	300	[17, 28]
	0.082	300	[9]
	0.079	300	This work
$(\alpha+\delta)/\delta$	0.926	300	[9]
	1.049	300	[17]
	1.013	300	This work

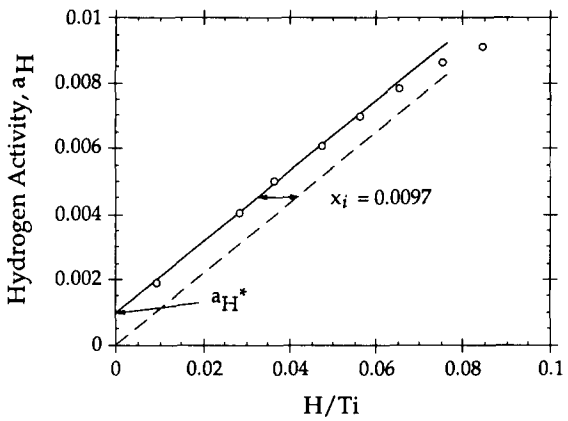

Fig. 4. Hydrogen activity *vs.* composition curve in the α solid solution region at 415 °C. Displacement is shown in the activity–composition correspondence, where an initial hydrogen activity a_H* was present. This displacement accounts for an initial hydrogen concentration (H:Ti) $x_i = 0.0097$.

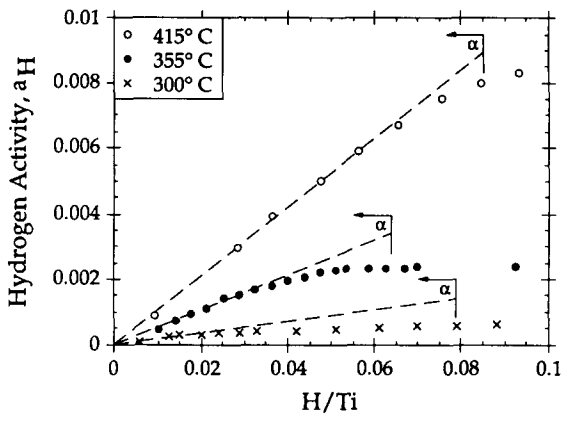

Fig. 5. Hydrogen activity *vs.* composition in the α solid solution region at 300, 355 and 415 °C. Dashed lines represent the values obtained by Sieverts' law. The α single-phase region at each temperature is displayed by an arrow.

primarily from an initial hydrogen concentration, as estimated using (11). This estimated initial concentration was then added to the hydrogen content introduced electrochemically to give the total hydrogen content. This total value was used in the data presented in Fig. 3 and related figures shown later. The same process was applied to the other two curves. The initial hydrogen concentration thus determined for 300, 355 and 415 °C are $x_i = 0.006$, 0.0105 and 0.0097 respectively.

3.4. Thermodynamic quantities

Figure 5 shows that the hydrogen activity varies with composition in the α phase solid solution region for each temperature. The linear relationship shown by each dashed line indicates that the respective system follows Sieverts' law in the dilute hydrogen concentration regime.

At 300 °C the hydrogen activity changes linearly with composition up to about H:Ti = 0.025 with $K_s = 0.0204$. At 355 and 415 °C a similar behavior persists until H:Ti ≈ 0.033 and 0.066 with $K_s = 0.0531$ and 0.104 respectively.

The Sieverts' constants obtained were then plotted against $1/T$ to determine the slope for the calculation of ΔH_H, as shown in Fig. 6. The value of ΔH_H calculated from (14) is -46.454 kJ mol^{-1} for the temperature range 300–415 °C. This value is listed in Table 2 to compare with those reported by others [9, 13, 15, 29].

The activity behavior for the β phase at 355 and 415 °C is different from that found in the α phase, as shown in Figs. 7 and 8. In the β single-phase region the curve indicates that the hydrogen activity gradually increases in an S-shaped fashion. There is an inflection point on each curve. The composition corresponding to the inflection point is $x \approx 0.66$ and 0.75 for 355 and 415 °C respectively.

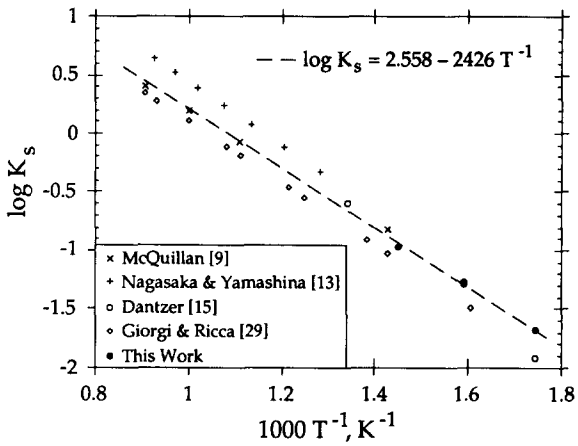

Fig. 6. Log K_s *vs.* $1/T$ curve of the Ti–H system. Results from other work [9, 13, 15, 29] are included for comparison. The slope leads to a value of ΔH_H of -46.454 kJ mol^{-1} in the range 300–415 °C.

TABLE 2. Comparison of partial molar enthalpies of hydrogen dissolution in the α-Ti solid solution region

ΔH_H (kJ (mol H)$^{-1}$)	Temperature range (°C)	Reference
−45.19	480–950	[9]
−52.72	500–800	[13]
$-40.17-34.31x$ $(0 \leqslant x \leqslant 0.0915)$[a]	464–473	[15]
$-41.84-45.56x$ $(0 \leqslant x \leqslant 0.09)$[b]	464	[15]
−50.63	350–800	[29]
−46.346	300	This work
−45.800	355	
−46.331 ($x = 0.02$)	415	
−46.454 $(0 \leqslant x \leqslant 0.025)$[c]	300–415	

[a]Data reported for ultrahigh purity titanium.
[b]Data reported for commercial titanium.
[c]From Figure 6 and eqn. (14).

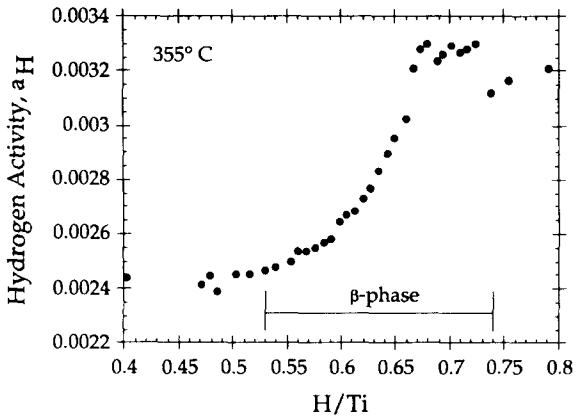

Fig. 7. Hydrogen activity *vs.* composition in the β phase hydride solution region at 355 °C.

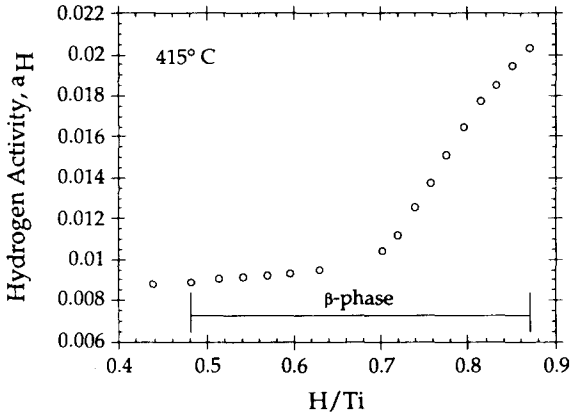

Fig. 8. Hydrogen activity *vs.* composition in the β phase hydride solution region at 415 °C.

The Gibbs free energy of formation, ΔG_f°, obtained from (4) for each single-phase region through the integration of the coulometric titration curve for three temperatures is shown in Fig. 9. Table 3(1) lists the equation from curve fitting, which represents the compositional dependence of the Gibbs free energy of formation for each phase at different temperatures. The extrapolated ΔG_f° value for the nominal composition "TiH_2" is shown to be -67.778 kJ mol^{-1} at 300 °C.

The free energy of reaction for the α-to-δ-hydride transformation at 300 °C and those for the α-to-β-hydride transformation at 355 and 415 °C are calculated from the respective Gibbs free energy of formation of the phases involved. Similarly, ΔG_r° can be obtained by (9) via the integration of the plateau potential over the two-phase composition range. Values from both methods are listed in Table 3(2) for comparison.

Figure 10 shows the compositional dependence of $\mathscr{E}^\circ$ in the α solid solution region. The dashed lines are constituted from the values calculated using (6) and (11). The resulting compositional dependence of $\mathscr{E}^\circ$ also allows us to calculate the partial molar free energy

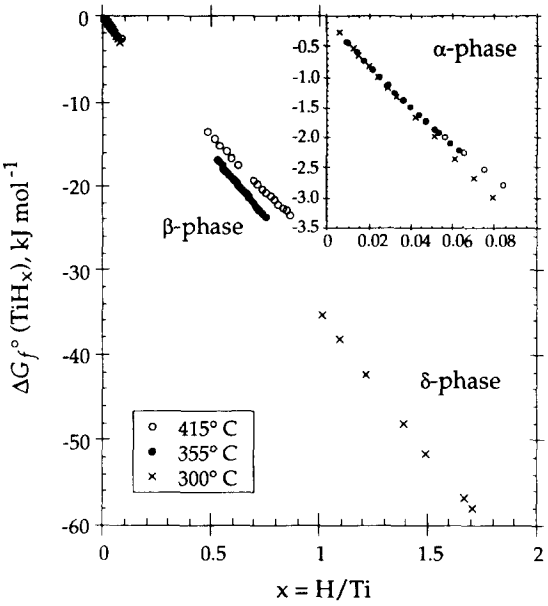

Fig. 9. Gibbs free energy of formation as a function of composition in the Ti–H system at 300, 355 and 415 °C.

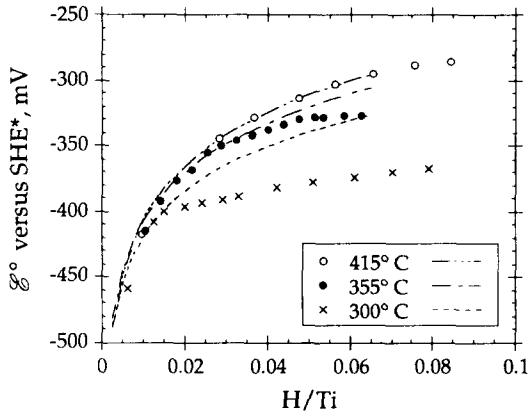

Fig. 10. Potential *vs.* composition curves in the α solid solution region of the Ti–H system. Dashed lines show the calculated $\mathscr{E}^\circ$ variation if Sieverts' law is followed at each temperature.

of mixing per mole of hydrogen, ΔG_H, using (6). Taking $x = 0.02$ as an arbitrary composition for this calculation, we obtain ΔG_H for the three temperatures and list them in Table 3(3).

As discussed in Section 2.3.5, by knowing the partial molar free energy of mixing per mole of hydrogen, ΔG_H, from coulometric titration measurements or fitted curves and by assuming that ΔH_H obtained from (14) is constant in the temperature range investigated, we estimated the partial molar entropy of mixing, ΔS_H, using (16). Figure 11 shows the ΔS_H results obtained from this method for each individual datum measured in coulometric titrations for the three temperatures. The values for $x = 0.02$ at the three temperatures are listed in Table 3(3).

TABLE 3. Thermodynamic quantities for phases and reactions in the Ti–H system

(1)	Phase	ΔG_f° (kJ mol^{-1})	T (°C)
	α ($0 \leqslant x \leqslant 0.079$)	$-0.084-37.113x$	300
	α ($0 \leqslant x \leqslant 0.063$)	$-0.151-33.456x$	355
	α ($0 \leqslant x \leqslant 0.085$)	$-0.221-31.107x$	415
	β ($0.53 \leqslant x \leqslant 0.74$)	$1.253-37.04x+5.14x^2$	355
	β ($0.48 \leqslant x \leqslant 0.87$)	$2.253-36.58x+8.00x^2$	415
	δ ($1.013 \leqslant x \leqslant 1.707$)	$-2.538-32.616x$	300
	TiH_2	-67.778	300

(2)	Reaction	ΔG_r° (kJ mol^{-1})		T (°C)
	$\alpha+0.934H=\delta$	-32.562[a]	-32.627[b]	300
	$\alpha+0.468H=\beta$	-14.675[a]	-14.768[b]	355
	$\alpha+0.395H=\beta$	-10.597[a]	-10.673[b]	415

(3)	Phase	ΔG_H (kJ (mol H)$^{-1}$)	ΔH_H (kJ (mol H)$^{-1}$)	ΔS_H (J (mol H)$^{-1}$ K^{-1})	T (°C)
	α ($x=0.02$)	-37.181	-46.582[c] (-46.454)	-16.407 (-16.183[d])	300
	α ($x=0.02$)	-35.755	-46.058[c] (-46.454)	-16.407 (-17.037[d])	355
	α ($x=0.02$)	-35.326	-46.614[c] (-46.454)	-16.407 (-16.174[d])	415

(4)	Composition	ΔG_f° (kJ mol^{-1})	ΔS_f° (J mol^{-1} K^{-1})	ΔH_f° (kJ mol^{-1})	T (°C)
	α ($x=0.02$)	-0.826	-0.182	-0.930	300
	α ($x=0.02$)	-0.820	-0.182	-0.934	355
	α ($x=0.02$)	-0.843	-0.182	-0.968	415

(5)	Reaction	ΔG_r° (kJ (mol H)$^{-1}$)	ΔS_r° (J (mol H)$^{-1}$ K^{-1})	ΔH_r° (kJ (mol H)$^{-1}$)	T (°C)
	α-to-β transformation	-31.357[a]	-67.544[e]	-73.774	355
	α-to-β transformation	-26.828[a]	-67.544[e]	-73.298	415

[a]Calculated from the corresponding ΔG_f°.
[b]Calculated from the plateau potentials (Table 5).
[c]Estimated from (16), in which $\Delta S_H = -16.407$ J (mol H)$^{-1}$ K^{-1} is obtained from (25) and assumed constant in the temperature range.
[d]Estimated from (22), in which $\Delta H_H = -46.454$ kJ (mol H)$^{-1}$ is obtained from (14) and assumed constant in the temperature range.
[e]Obtained from the slope of the broken line in Fig. 12, plateau potential measurements based on per mole of hydrogen.

Alternatively, we obtained temperature-dependent $\mathscr{E}^\circ$ from ΔG_H (from the fitted curves at $x=0.02$) for the calculation of ΔS_H using (25). When an $\mathscr{E}^\circ$ *vs.* T curve was plotted, the slope was used to calculate the ΔS_H value. The values for other hydrogen concentrations using the same calculation are also displayed in Fig. 11. By assuming a constant ΔS_H at $x=0.02$ over the entire temperature range, we subsequently calculated ΔH_H using (16). The results from this calculation are also listed in Table 3(3).

ΔS_H values were also calculated from (17). The k values were determined by K_s and ΔH_H using (13), (18) or (19). The k values for 300, 355 and 415 °C are 350.12, 387.99 and 349.79 respectively. The ΔS_H values obtained in this way are presented in Fig. 11 as broken lines for each temperature.

The integral molar entropy of formation, ΔS_f°, which was obtained from (23) on a per mole of hydrogen basis for the α solid solution region, is shown in Fig. 11. This is of course based upon the assumption of a constant $\partial\mathscr{E}^\circ/\partial T$ over the temperature range studied. Similarly, we obtained $\Delta S_f^\circ(TiH_x)$ on a per mole of TiH_x basis. Knowing $\Delta G_f^\circ(TiH_x)$, we estimated $\Delta H_f^\circ(TiH_x)$ using $\Delta H_f^\circ = \Delta G_f^\circ + T\Delta S_f^\circ$, as Table 3(4) shows.

The integral molar quantities of mixing, ΔG_m, ΔS_m and ΔH_m, can be obtained through (5), (24) and $\Delta H_m = \Delta G_m + T\Delta S_m$ respectively. Their values can be readily calculated from the formation data in Figs. 9 and 11 and Table 3(4).

The entropy of reaction, ΔS_r°, which corresponds to the α-to-β-hydride transformation was obtained according to (20). The temperature dependence of the plateau potential was obtained from the experiments described in Section 2.2. Figure 12 displays the $\mathscr{E}^\circ$ *vs.* T curve. The plateau potentials obtained from the

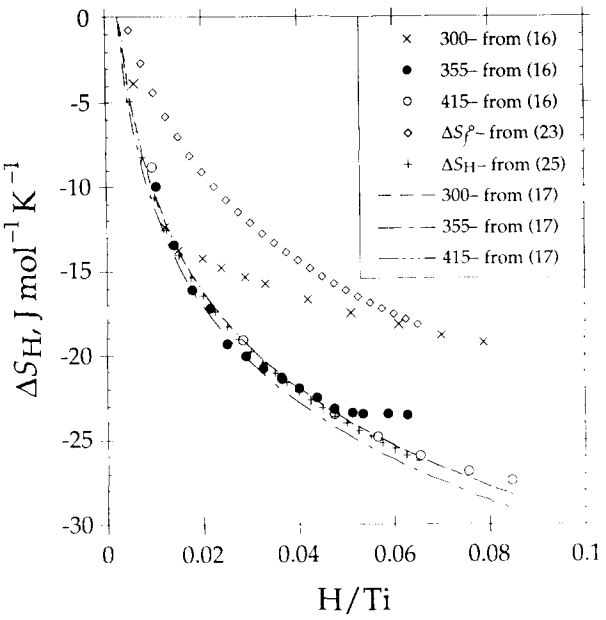

Fig. 11. Partial molar entropy of mixing of hydrogen, ΔS_H, and integral molar entropy of formation, ΔS_f°, as a function of composition in the α solid solution region.

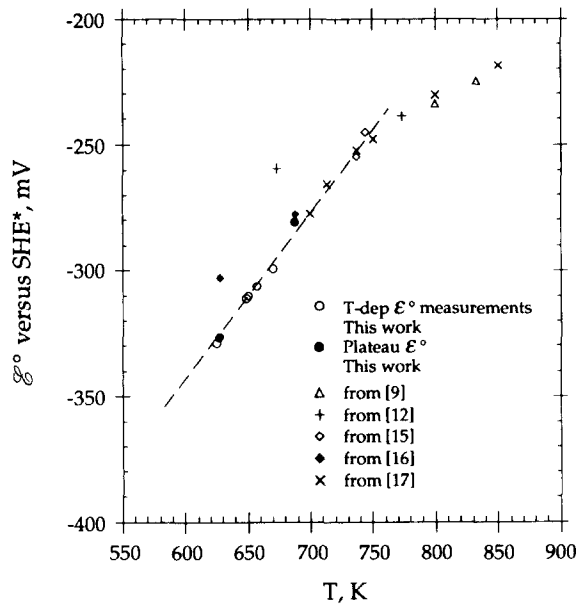

Fig. 12. Temperature dependence of plateau potential for the two-phase $\alpha+\beta$ region in the Ti–H system. Two sets of data from this work are shown: open circles are from direct measurements of plateau potential at various temperatures; solid circles are taken from coulometric titration curves. Data from various reports [9, 12, 15–17] are included for comparison. The slope was used to calculate the ΔS_r° value listed in Table 3(5).

coulometric titration measurements at 355 and 415 °C are also shown, in addition to some values calculated from the equilibrium partial pressures determined from the p–c–T curves at similar or higher temperatures reported in refs. 9, 12 and 15–17. The linear relationship shown by this curve allows us to calculate ΔS_r° from the slope. A value of -67.544 J mol^{-1} K^{-1} for 300–470 °C is listed in Table 3(5) for the estimation of ΔH_r° using (21).

TABLE 4. Comparison of partial molar energies of mixing of titanium in the α solid solution region

Composition x	ΔG_{Ti} (J mol^{-1})	T (°C)	Reference
0.05	−305	441	[9]
	−237	333	
	−299	415	This work
	−226	355	
0.07	−453	441	[9]
	−346	333	
	−420	415	This work
	−339	355	

From the coulometric titration curves and the derived free-energy curves we can deduce the partial molar free energy of mixing for titanium, ΔG_{Ti}, in the α solid solution region using (7). The values for two compositions, $x=0.05$ and 0.07, are listed in Table 4 for comparison with values reported by McQuillan [9]. A considerably good agreement is obtained.

4. Discussion

4.1. Initial hydrogen concentration

We attributed the initial hydrogen concentration to various sources, according to how we found the displacement between a_H and x in the α solid solution region in Fig. 4. When the titanium sample was placed for electrochemical measurements, LiH in the electrolyte would react with surface oxides to produce clean metal surfaces and evolve hydrogen. Some of the hydrogen evolved was inevitably absorbed by the titanium during this process, leading to the initial hydrogen content in the samples. Another source for the initial hydrogen content could result from the residual hydrogen trapped in the lattice and retained after subsequent sample treatments. The residual hydrogen could come from preparation methods or from the reaction between the purified titanium sample and moisture upon exposure to the air. Subsequent decomposition of moisture into oxide and hydrogen could initially introduce hydrogen to the sample.

4.2. Phase relationships and phase boundaries

The phase relationships and boundaries obtained by the coulometric titration are consistent with the newly reported phase diagram by San-Martin and Manchester [17] shown in Fig. 1, which indicates that a eutectoid reaction, $\beta=\alpha+\delta$, occurs at about 300 °C, although some early work showed a eutectoid temperature at 315 °C [9] or even higher [12] and some reported a

lower temperature at 281 °C [16]. Below 300 °C the Ti–H system has only a two-phase $\alpha+\delta$ region. Above this eutectoid temperature the β phase exists and two two-phase regions, $\alpha+\beta$ and $\beta+\delta$, are present.

The hydrogen concentrations at the phase boundaries are compared in Table 1 with reported results from refs. 9, 15, 17 and 24–28 which were obtained by X-ray diffraction, electrical resistivity and nuclear magnetic resonance methods. Generally the data are in a good agreement within experimental error. However, we did not discuss the effect of stress and the associated defect densities on the hydrogen solubility. This effect could make a significant contribution to the discrepancies among the studies.

4.3. Plateau potentials

The potential of the two-phase $\alpha+\delta$ plateau is at -362 mV(SHE*) at 300 °C. The two-phase $\alpha+\beta$ plateau lies at -327 and -280 mV, while the $\beta+\delta$ plateau is estimated to be at -310 and -230 mV at 355 and 415 °C respectively. We compared the coulometric titration results with those taken from the volumetric p–c–T curves reported in ref. 17 for the same temperature range but at higher partial pressures (Fig. 3). The correlation is excellent. The linear behavior of the temperature-dependent plateau potential in Fig. 12 demonstrates the consistency between our electrochemical technique and gas-volumetric methods reported by others [9, 12, 15, 16] in Table 5.

TABLE 5. Plateau potentials measured by different techniques in the Ti–H system

Two-phase plateau	Potential (mV (SHE*))	T (°C)	Reference
$\alpha+\beta$	−234	527	[9]
	−225	560	
	−238	500	[12]
	−259	400	
	−255	464	[15]
	−245	471	
	−303	355	[16]
	−278	415	
	−327	355	This work
	−280	415	
$\beta+\delta$	−144	500	[12]
	−202	400	
	−168	464	[15]
	−310	355	This work
	−230	415	
$\alpha+\delta$	−324	300	[12]
	−362	300	This work

*Refers to $H^- = \frac{1}{2}H_2 + e^-$ reversible reaction.

4.4. Sieverts' law

Figure 5 shows that the hydrogen activity is consistent with Sieverts' law (dashed lines) in the dilute solid solution region. The K_s values obtained at the three temperatures are compared with those extracted from other studies [9, 13, 15, 29] in Fig. 6. The values of McQuillan [9] and Dantzer [15] fall on a linear curve drawn through the values measured in this work. However, the values of Nagasaka and Yamashina [13] and Giorgi and Ricca [29] fall on two separate linear curves which are almost parallel to ours. The consistency in the slopes of the various sets of data indicates good agreement in the enthalpy values, as will be discussed next. We also demonstrated that to obey Sieverts' law we have to consider the initial hydrogen concentration.

4.5. Other thermodynamic behaviors

4.5.1. Free energies

The value of ΔG_f° for TiH_2 at 300 °C was estimated to be -67.778 kJ mol^{-1} from our coulometric titration results (Table 3(1)). Arita *et al.* [14] reported values in the range 404–606 °C. An extrapolation to 300 °C gives -58.101 kJ mol^{-1}. From the thermochemical data reported by Stull and Prophet [30] we obtained a value of -69.375 kJ mol^{-1} at 300 °C. A value of $\Delta G_f^\circ = -63.361$ kJ mol^{-1} at 327 °C was calculated from free-energy values in ref. 31. The last two results agree well with our data.

Table 3(1,2) lists the integral molar free energies for different phases and reactions. Using Giorgi and Ricca's reported hydrogen partial pressure values in the low concentration region obtained from their ultrahigh vacuum studies [29],

$$\ln(P_{H_2},(\text{atm})) = 12.653 + \ln(\text{H:Ti})^2 - \frac{12174}{T} \qquad (26)$$

we calculated $\Delta G_H = -39.108$, -38.004 and -36.799 kJ mol^{-1} for $x = 0.02$ at 300, 355 and 415 °C respectively. We also extrapolated their concentration-dependent ΔG_H for hydrogen solution at 500 °C and a value of -35.091 kJ mol^{-1} was obtained. These results agree with our reported values in Table 3(3).

4.5.2. Enthalpies

The value of ΔH_H calculated from (14) using the slope of the log K_s *vs.* $1/T$ curve shown in Fig. 6 is -46.454 kJ mol^{-1} for hydrogen dissolution in the α solid solution region. This value is listed in Tables 2 and 3(3) to compare with the results reported by others [9, 13, 15, 29] and the data obtained using alternative calculations. Excellent agreement is obtained, especially with those previously reported in refs. 9 and 29. Using the composition $x = 0.02$ as an example, Dantzer's values would be -40.86 and -42.75 kJ mol^{-1} for highly pure and commercial titanium respectively at 464 °C; our

value is -46.331 kJ mol^{-1} at 415 °C. The values obtained by various authors seem to be sensitive to the material's purity and treatment. The integral molar enthalpy of formation, ΔH_f, reported by Dantzer *et al.* [24] is -0.920 kJ mol^{-1} for $x=0.02$ at 714 K (441 °C). Our values in Table 3(4) agree well.

4.5.3. Entropies

According to Giorgi and Ricca's formula for partial molar entropies of solution,

$$(\Delta S)_{H_2} = -12.573 + \tfrac{1}{2}R \ln(\mathrm{H{:}Ti})^2 \text{ (e.u./g-atom)} \quad (27)$$

we calculated $\Delta S_H = -20.082$ J mol^{-1} K^{-1}, which is more negative than our values in Table 3(3). Dantzer *et al.* [24] reported concentration-dependent entropy values, which led to the calculation of

$$\Delta S_H = \frac{\Delta H_H - \Delta G_H}{T} = S_H - \tfrac{1}{2}S_{H_2}^{\circ} \quad (28)$$

The S_H values were reported in their work and the $S_{H_2}^{\circ}$ values can be obtained from ref. 31. We estimated $S_H = 13.2$ cal mol^{-1} K^{-1} at $x \approx 0.02$ at 721 K (448 °C). The $S_{H_2}^{\circ}$ value at 700 K is 37.143 cal mol^{-1} K^{-1} [31]. Taking 1 cal = 4.184 J, a value of ΔS_H on the order of -22.5 J mol^{-1} K^{-1} was obtained. The ΔG_H and ΔH_H values used in their and our studies largely corresponded to this noted difference.

The behavior of the partial molar entropy of solution exhibits interesting implications in describing the hydrogen dissolution in a metal lattice. Near infinite dilution the value of ΔS_H is positive owing to a significant contribution from the configurational entropy as discussed in Section 2.3.4. This view coincides with the conventional "lattice gas model" and Sieverts' law, which are typically used in describing the hydrogen dissolution behavior in the dilute solid solution region. As the hydrogen concentration increased in the lattice, ΔS_H became more and more negative, implying an increasingly more ordered state than in the gas phase (Fig. 11). The increasing ordering of hydrogen in the lattice with hydrogen concentration seems to deviate from the "lattice gas model" and Sieverts' law. This behavior could stem from an increasing elastic H–H attractive interaction through lattice relaxation, which leads to the compositional dependence of entropies and enthalpies. However, this ordering behavior was not discussed previously by others in terms of crystal structural evidence nor by theoretical prediction. It remains an interesting aspect for future study.

Van Mal [32] considered that the entropy change of reaction, ΔS_r, during a hydride phase transformation is typically invariant with temperature. To a first-order approximation he proposed a characteristic $-7.5R$ or -62.36 J mol^{-1} K^{-1} value for ΔS_r. This is close to our reported value listed in Table 3(5) for the α-to-β transformation. It should be noted that this value is based on one mole of hydrogen atoms. The value is almost insensitive to the M–H system or the type of phase transformation.

4.5.4. β-Hydride phase

The activity behavior in the β-hydride phase region exhibits an inflection point at $x \approx 0.66$ and 0.75 for 355 and 415 °C respectively (Figs. 7 and 8). The inflection point is often referred to as the stoichiometric composition of the single phase [33]. Therefore $TiH_{0.66}$ and $TiH_{0.75}$ were considered to be the stoichiometric composition of the β phase at the respective temperature, in comparison with the eutectoid composition $TiH_{0.639}$. The increase in the stoichiometric composition with temperature is worth noting. This behavior seems to follow the solidus line along the $\beta/(\beta+\delta)$ boundary, as Fig. 1 exhibits. The dissolved hydrogen is usually considered to occupy the tetrahedral T sites in the β b.c.c. lattice. There are six T sites per titanium atom in the unit cell. The composition variation indicates that the occupancy ratio increased from 11% to 12.5% in a 60 °C interval, assuming completely random occupation of the T sites. An interesting question would be "does the stoichiometric composition have any structural meaning?". Although there is no report on any ordered phase in the β phase region, the question remains of a possibility of mixed occupancy between tetrahedral (T) and octahedral (O) sites.

5. Conclusions

A novel electrochemical technique has been reported for the investigation of the thermodynamic properties of the Ti–H system. The method employs alkali halide molten salt electrolytes containing LiH and appropriate reference electrodes in a simple electrochemical cell arrangement. Experiments were conducted in a much lower pressure and temperature regime than is possible by the use of the conventional gas-volumetric absorption method. It was shown that thermodynamic information can be determined quite readily by the use of these electrochemical techniques. The data collected from the equilibrium coulometric titration curves can be used to reveal the phase relationships, phase boundary compositions, hydrogen activity changes in different phases and various other thermodynamic quantities.

Acknowledgment

The authors would like to thank the US Department of Energy for its financial support under subcontract LBL-4536310.

References

1 J. J. Reilly, *Z. Phys. Chem., 117* (1979) 155.
2 R. Wiswall, in G. Alefeld and J. Völkl (eds.), *Topics in Applied Physics,* Vol. 29, *Hydrogen in Metals II,* Springer, Berlin, 1978, Chap. 5, p. 201.
3 P. S. Rudman and G. D. Sandrock, *Ann. Rev. Mater. Sci., 12* (1982) 271.
4 H. Buchner, in A. F. Andresen and A. J. Maeland (eds.), *Proc. Int. Symp. on Hydrides for Energy Storage, Geilo,* Pergamon, London, 1978, p. 569.
5 B. Y. Liaw, G. Deublein and R. A. Huggins, in D. R. Turner (ed.), *Proc. Symp. on Chemical Sensors, 172nd Electrochemical Society Meeting, Honolulu, HI, 1987,* Vol. 87-9, Electrochemical Society, NJ, 1987, p. 91; *Solid State Ionics, 28–30* (1988) 1660.
6 D. W. Jones, N. Pessall and A. D. McQuillan, *Philos. Mag., [8] 6* (1961) 455.
7 W. M. Mueller, J. P. Blackledge and G. G. Libowitz, *Metal Hydrides,* Academic, London, 1968.
8 L. Kirschfeld and A. Sieverts, *Z. Phys. Chem. A, 145* (1929) 227.
9 A. D. McQuillan, *Proc. R. Soc. Lond. A, 204* (1950) 309.
10 T. R. P. Gibb Jr. and H. W. Kruschwitz Jr., *J. Am. Chem. Soc., 72* (1950) 5365.
11 T. R. P. Gibb Jr., J. J. McSharry and R. W. Bragdon, *J. Am. Chem. Soc., 73* (1951) 1751.
12 R. M. Haag and F. J. Shipko, *J. Am. Chem. Soc., 78* (1956) 5155.
13 M. Nagasaka and T. Yamashina, *J. Less-Common Met., 45* (1976) 53.
14 M. Arita, K. Shimizu and Y. Ichinose, *Metall. Trans. A, 13* (1982) 1329.
15 P. Dantzer, *J. Phys. Chem. Solids, 44* (1983) 913.
16 E. Veleckis and A. G. Rogers, *J. Less-Common Met., 97* (1984) 79.
17 A. San-Martin and F. D. Manchester, *Bull. Alloy Phase Diag., 8* (1987) 30, and references cited therein.
18 C. M. Lüdecke, G. Deublein and R. A. Huggins, in T. N. Veziroglu and J. B. Taylor (eds.), *Hydrogen Energy Progress V,* Pergamon, NY, 1984, p. 1421.
19 C. M. Lüdecke, G. Deublein and R. A. Huggins, *J. Electrochem. Soc., 132* (1985) 52.
20 C. M. Lüdecke, G. Deublein and R. A. Huggins, *Int. J. Hydrogen Energy, 12* (1987) 81.
21 G. Deublein and R. A. Huggins, *J. Electrochem. Soc., 136* (1989) 2234.
22 W. Weppner and R. A. Huggins, *J. Electrochem. Soc., 125* (1978) 7.
23 T. B. Flanagan and W. A. Oates, *Ber. Bunsenges. Phys. Chem., 76* (1972) 706.
24 P. Dantzer, O. J. Kleppa and M. E. Melnichak, *J. Chem. Phys., 64* (1976) 139.
25 R. M. Gabidulin, B. A. Kolachev, A. A. Bukhanova and E. V. Shchekoturova, in A. Belov (ed.), *Proc. 3rd Int. Conf. on Titanium and Titanium Alloys: Scientific and Technological Aspects, Moscow, 1976,* Vol. 2, 1978, p. 419 (in Russian); Engl. transl.: W. J. Case (ed.), Vol. 2, Plenum, New York, 1982, p. 1365.
26 R. L. Beck, *Summary Rep. USAEC Rep. LAR-10,* 1960, pp. 60–65, 77–80 (Denver Research Institute).
27 G. A. Lenning, C. M. Craighead and R. I. Jaffee, *Trans. Metall. AIME, 200* (1954) 367.
28 R. S. Vitt and K. Ono, *Metall. Trans., 2* (1971) 608.
29 T. A. Giorgi and F. Ricca, *Nuovo Cimento (Suppl.), 5* (1967) 472.
30 D. R. Stull and H. Prophet, *JANAF Thermochemical Tables,* NSRDS-NBS 37, US Government Printing Office, Washington, DC, 2nd edn., 1971.
31 I. Barin, O. Knacke and O. Kubaschewski, *Thermochemical Properties of Inorganic Substances,* Springer, Berlin, 1973; Suppl., 1977.
32 H. H. van Mal, Stability of ternary hydrides and some applications, *Ph.D. Thesis,* Technische Hogeschool, Delft, 1976, p. 92.
33 C. Wager and W. Schottky, *Z. Phys. Chem. B, 11* (1931) 163.